Fournier and Forand (1994) derived an approximate analytic form for the phase function of an ensemble of particles that have a hyperbolic (Junge) particle size distribution, with each particle scattering according to the anomalous diffraction approximation to the exact Mie theory . [For a hyperbolic or Junge cumulative size distribution, the number $N(r)$ of particles per unit volume with size greater than r (volume-equivalent spherical radius) is proportional to $r^{-\mu}$, so that $-\mu$ is the slope of the size distribution when $\log N(r)$ is plotted vs $\log r$. Oceanic particle size distributions typically have μ values between 3 and 5.] In its latest form (Fournier and Jonasz, 1999) this phase function is given by

$$\tilde{\beta}_{\mathrm{FF}}(\psi) = \&\frac{1}{4\pi(1-\delta)^2\delta^\nu}\left[\nu(1-\delta) - (1-\delta^\nu) + [\delta(1-\delta^\nu) - \nu(1-\delta)]\,\sin^{-2}\left(\frac{\psi}{2}\right)\right] \quad (1)$$
$$+\&\frac{1-\delta_{180}^\nu}{16\pi(\delta_{180}-1)\delta_{180}^\nu}(3\cos^2\psi - 1)\,,$$

where

$$\nu = \frac{3-\mu}{2} \quad \text{and} \quad \delta = \frac{4}{3(n-1)^2}\,\sin^2\left(\frac{\psi}{2}\right)\,. \quad (2)$$

Here n is the real index of refraction of the particles, μ is the slope parameter of the hyperbolic distribution, and δ_{180} is δ evaluated at $\psi = 180$deg. Equation (1) can be integrated to obtain the backscatter fraction,

$$B = \frac{b_b}{b} = 1 - \frac{1 - \delta_{90}^{\nu+1} - 0.5(1-\delta_{90}^\nu)}{(1-\delta_{90})\delta_{90}^\nu}\,, \quad (3)$$

where δ_{90} is δ evaluated at $\psi = 90$ deg. Although Eq. (2) uses only the real part of the index of refraction, the addition of moderate amounts of absorption does not significantly change the shape of the phase functions generated by Eq. (1).

Figures figure1 and figure2 show Fournier-Forand phase functions for a wide range of B values; each curve is labeled by its backscatter fraction. Most oceanic particles have backscatter fractions between $B = 0.001$ (e.g., very large phytoplankton) and 0.1 (e.g., very small mineral particles). Table center1 shows the n and μ values used in Eqs. (1) and (2) to obtain these curves.

index ofrefraction n **& Junge slope** μ **& backscatter fraction** B
1.021 & 3.0742 & 0.0001
1.040 & 3.2010 & 0.001
1.08 & 3.483 & 0.01
1.175 & 4.065 & 0.1
1.15 & 4.874 & 0.4

Table 1: The n and μ values used in Eqs. (1) and (2) to generate the Fournier-Forand phase functions of Figs. figure1 and figure2.

Figures figure3 and figure4 show how well the Fournier-Forand phase function can reproduce the shapes of measured phase functions for the types of particles found in ocean water.

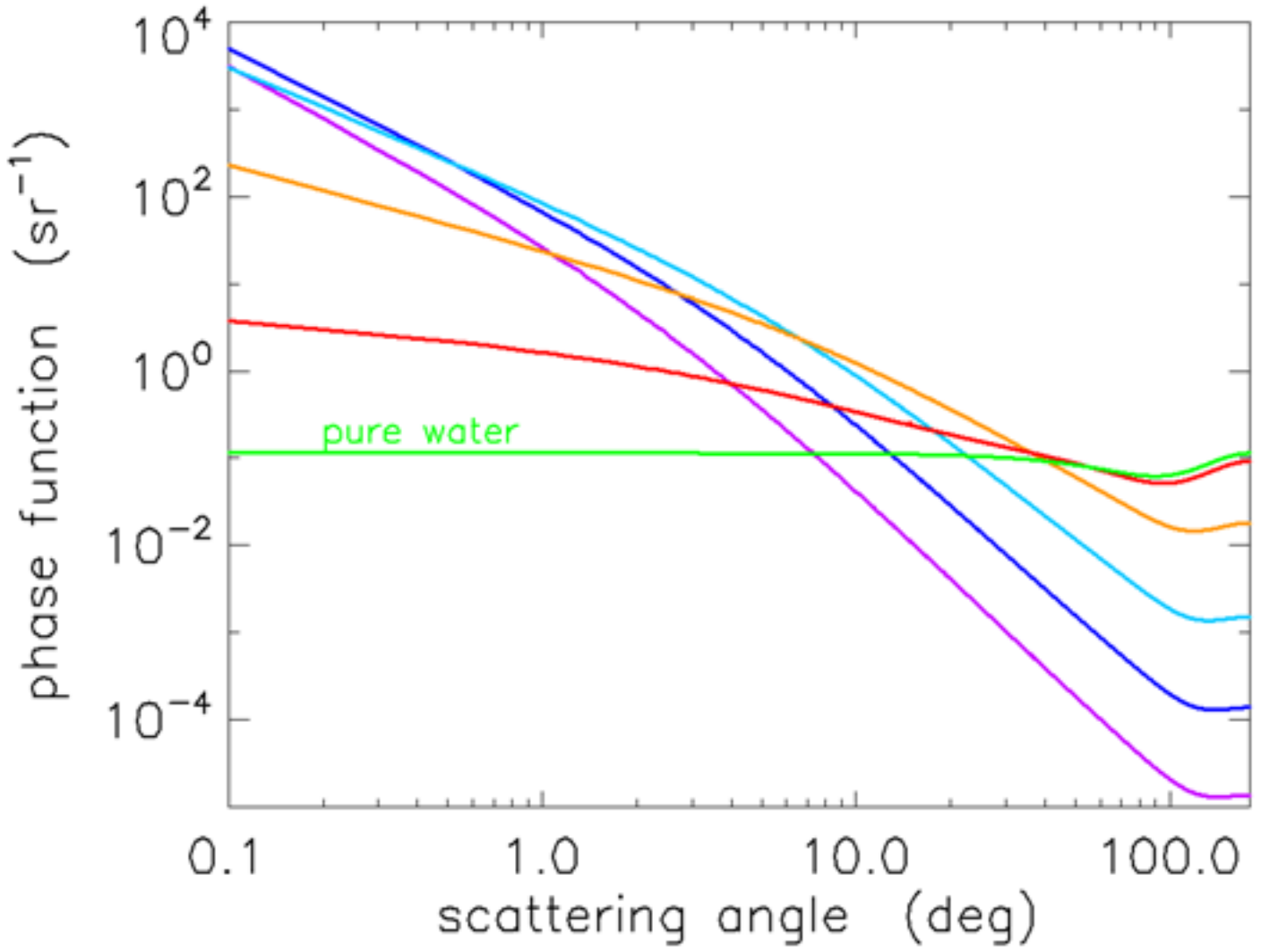

Figure 1: Log-log plot of Fournier-Forand phase functions for selected backscatter fractions B. The green curve is the pure sea water phase function, which has $B = 0.5$.

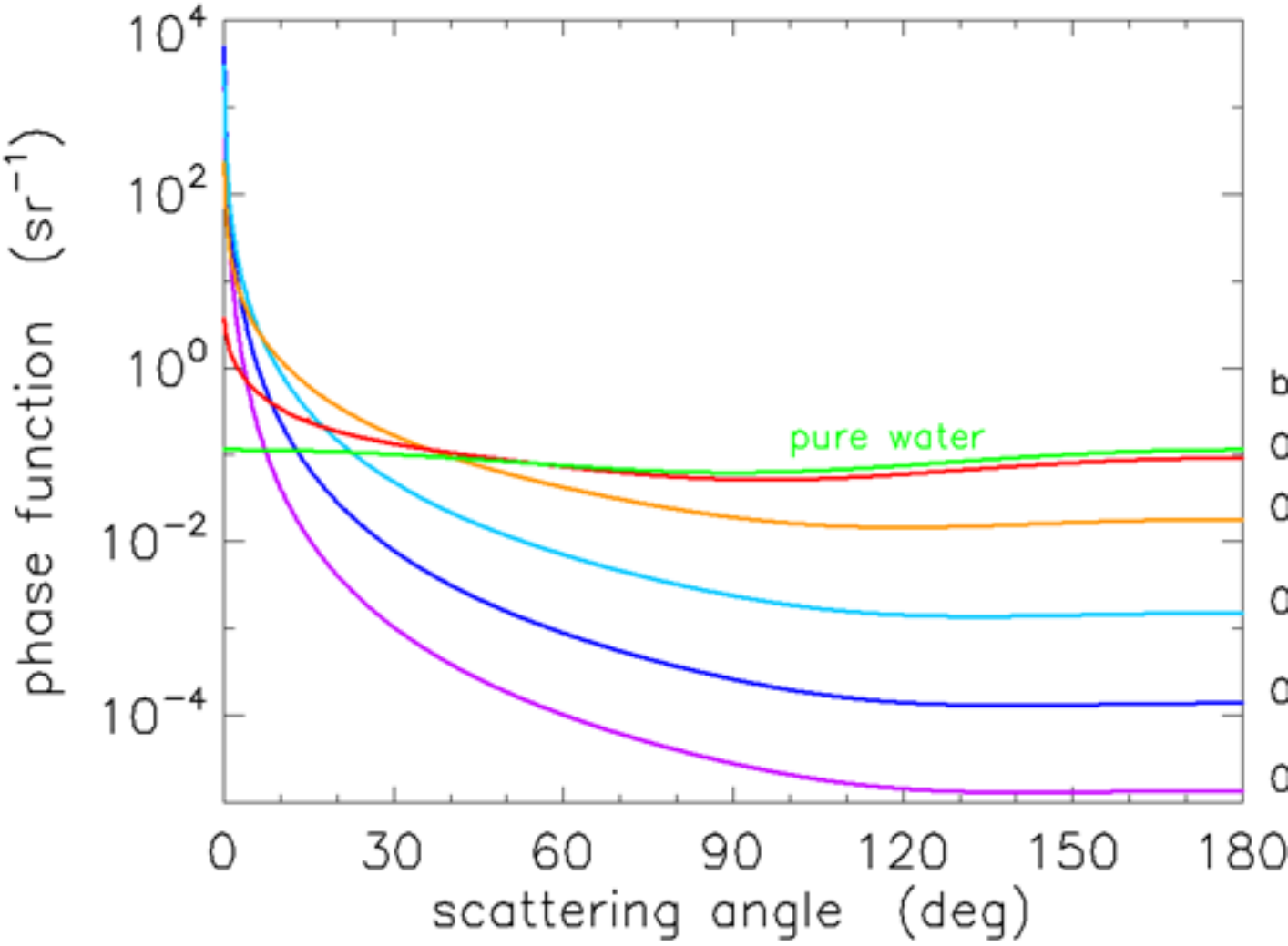

Figure 2: Log-linear plot of Fournier-Forand phase functions for selected backscatter fractions B. The green curve is the pure sea water phase function, which has $B = 0.5$.

In those figures, the blue curves are three phase functions measured by the Volume Scattering Meter (VSM) of Lee and Lewis (2003), and the green curve is the Petzold average-particle phase function. The red curves show the Fournier-Forand phase functions with the same backscatter fractions as the measured phase functions. Each pair of measured and FF phase functions is labeled by the backscatter fraction B in Fig. figure4.

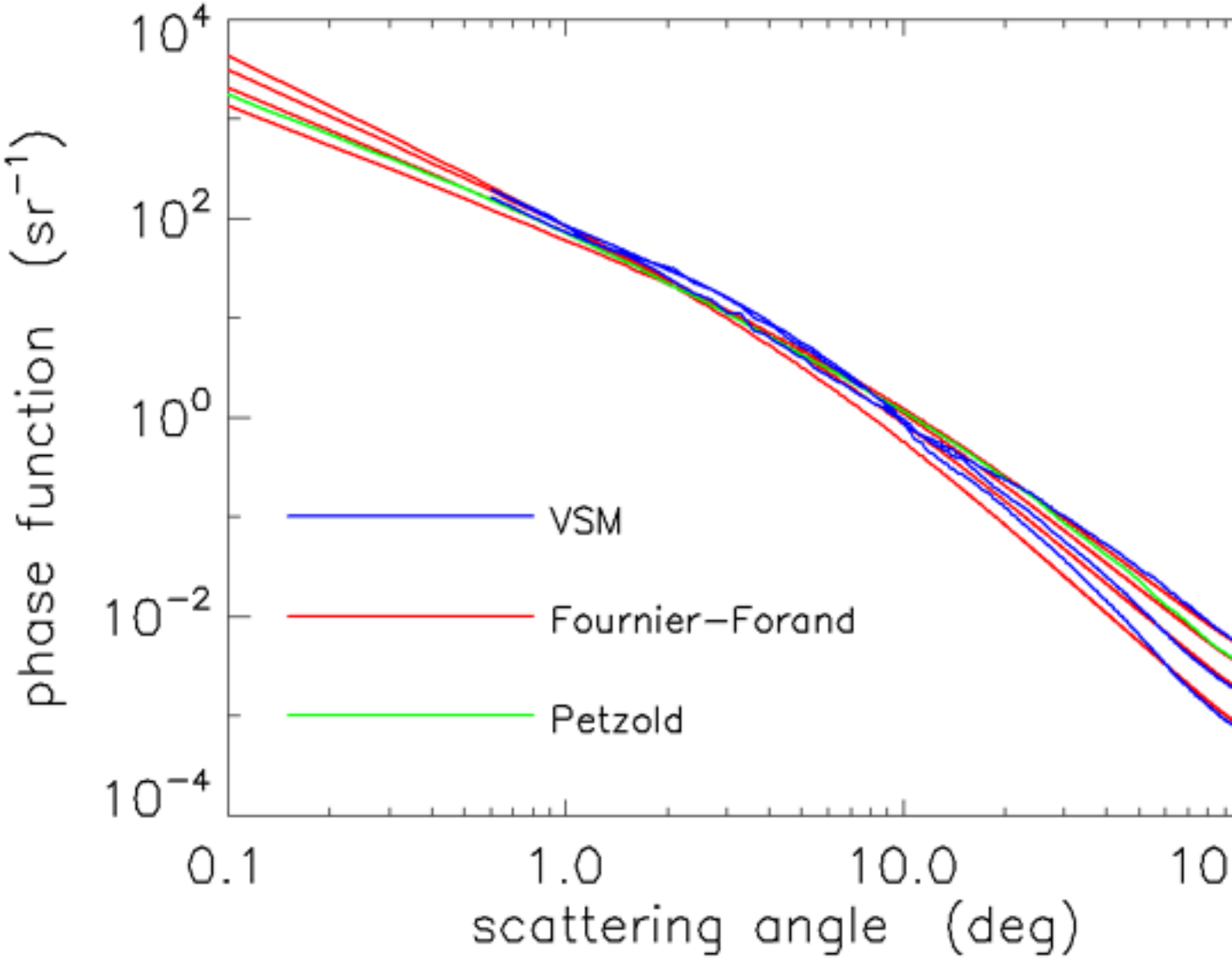

Figure 3: Log-log plot of 4 measured phase functions (blue and green curves), and the Fournier-Forand phase functions with the same backscatter fractions (red curves).

As seen in Figs. figure3 and figure4, the Fournier-Forand analytical model does a much better job of reproducing the shapes of ocean phase functions than does the Henyey-Greenstein phase function (or any other previously developed analytical model), especially at very small angles. There is considerable discrepancy between the measured and modeled VSM data at wavelengths near 180 deg, but it is not known how much of this may be due

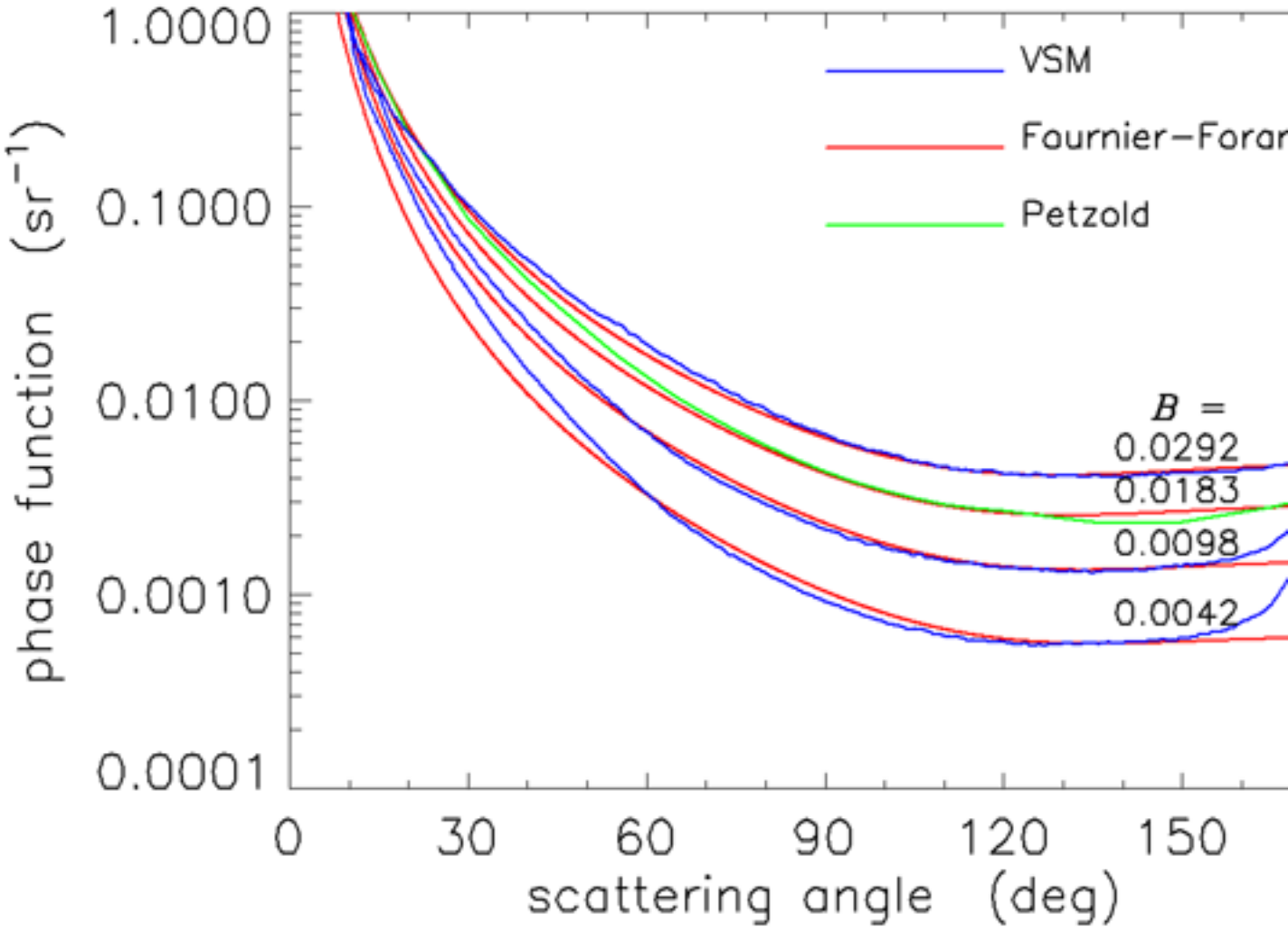

Figure 4: Log-linear plot of 4 measured phase functions (blue and green curves), and the Fournier-Forand phase functions with the same backscatter fractions (red curves).

to instrumental error. In any case, Fournier-Forand phase functions give the best fits to measurements of any analytical model yet developed. They therefore are now commonly used in numerical simulations (e.g., in HydroLight) and have replaced other analytic models for oceanographic simulations. The light fields resulting from the use of Fournier-Forand and several other measured and modeled phase functions in numerical simulations are compared in Mobley et al. (2002).

The relation between n, μ, and B is not unique. Figure figure5 shows selected backscatter values given by Eq. (3) as a function of n and μ. The red dot on the $B = 0.0183$ curve shows the values of $n = 1.10$ and $\mu = 3.5835$ for which Eq. (1) gives the best fit to the Petzold average-particle phase function, as seen in Figs. figure3 and figure4. However, any pair of n and μ values lying on a curve of constant B in Fig. figure5 will generate a slightly different phase function having the given B value. The phase functions corresponding to the two red squares and the red dot on the $B = 0.0183$ contour give the phase functions shown in Figs. figure6 and figure7. These functions have somewhat different shapes, but any is still a reasonable approximation to the Petzold average particle phase function shown in red in those figures. Thus the exact n and μ values used to generate a Fournier-Forand phase function with a given backscatter fraction are not critical for most applications.

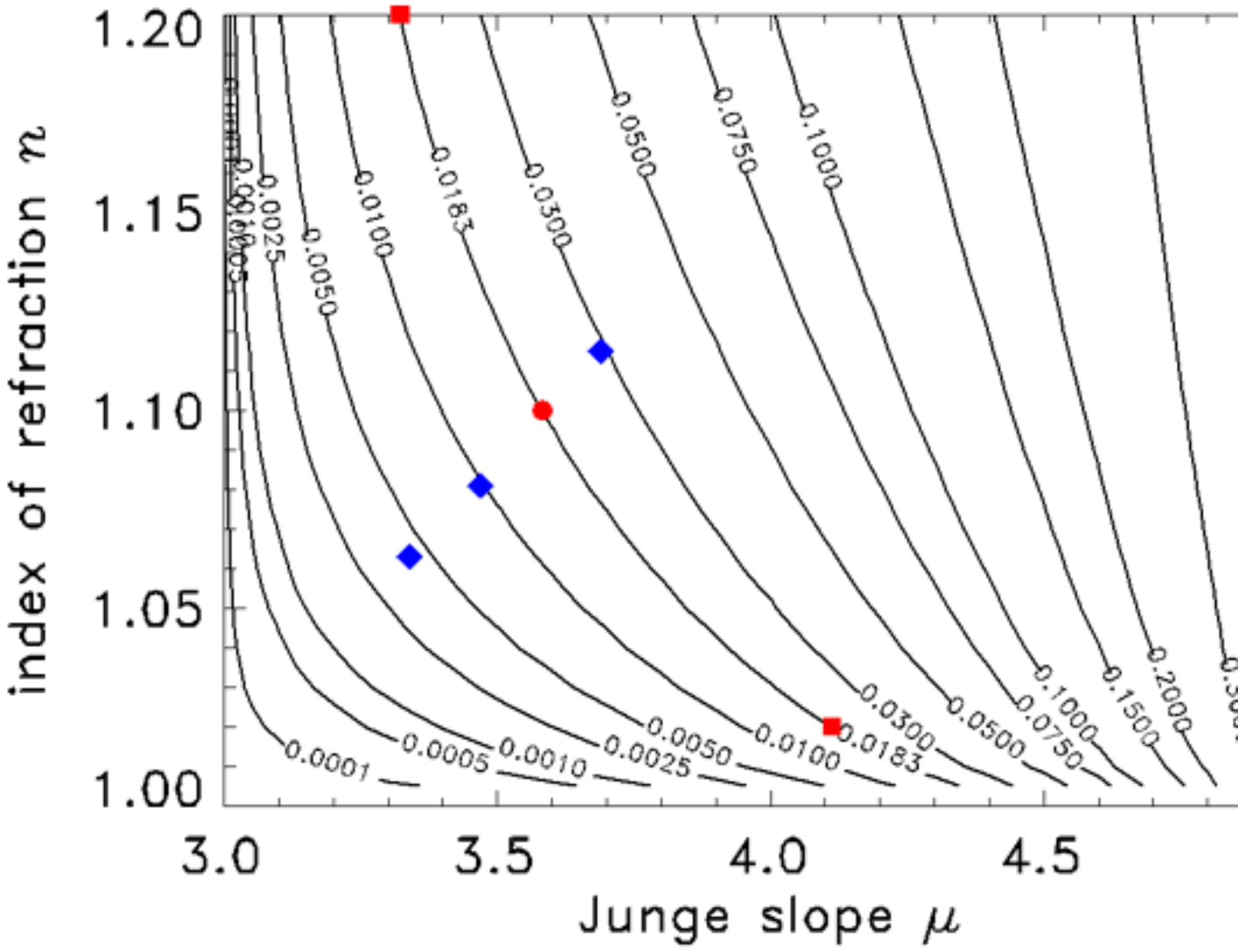

Figure 5: The Fournier-Forand backscatter fraction as a function of index of refraction and Junge slope. The red dot shows and the blue diamonds give the n and μ value used to generate the phase functions of Figs. figure3 and figure4. The red symbols show the values used to generate the phase functions with $B = 0.0183$ shown in Figs. figure6 and figure7.

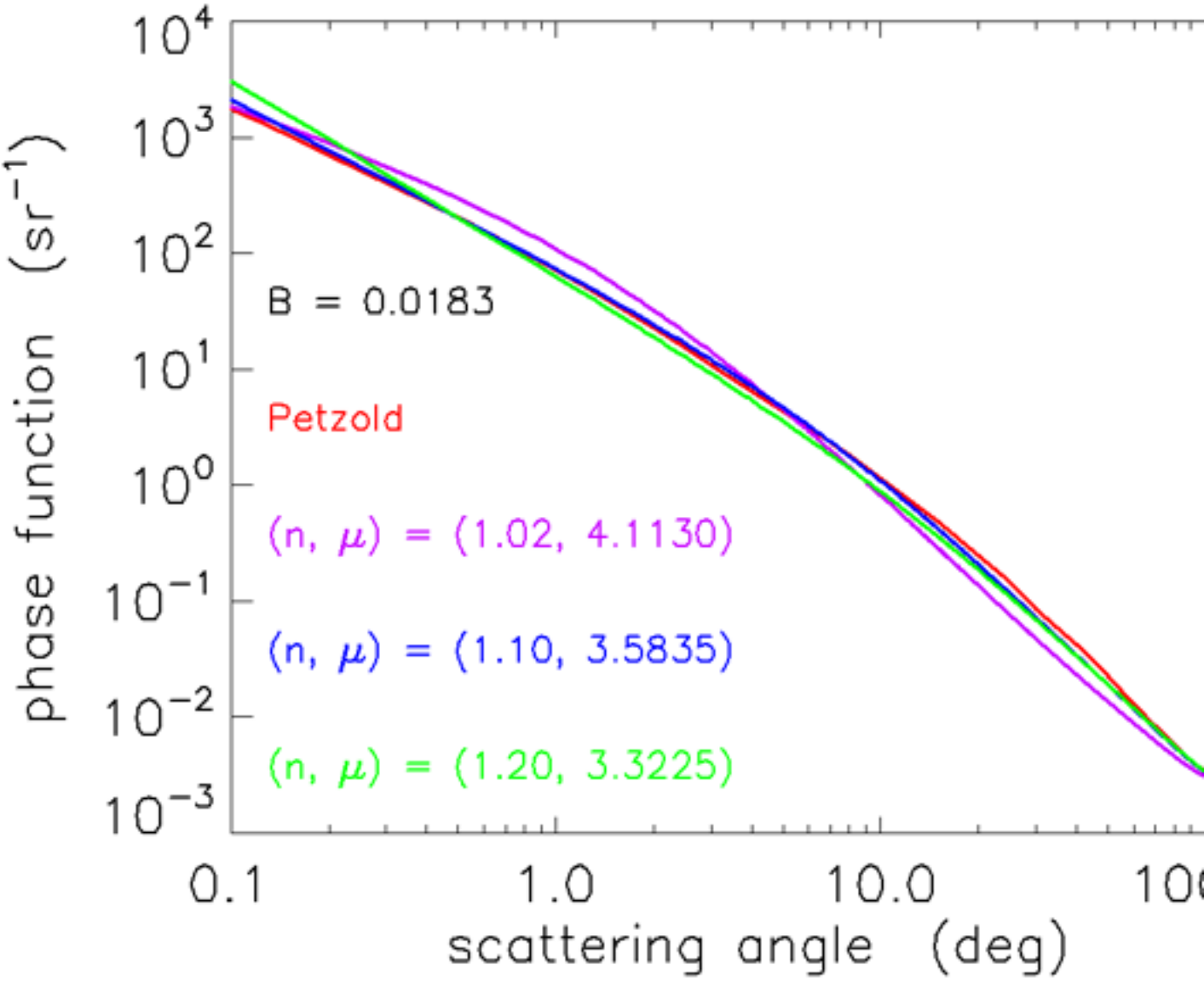

Figure 6: Log-log plots of Fournier-Forand phase functions having the same backscatter fraction $B = 0.0183$ but generated by the three n, μ pairs shown by the red symbols in Fig. figure5. The Petzold average-particle phase function is shown in red.

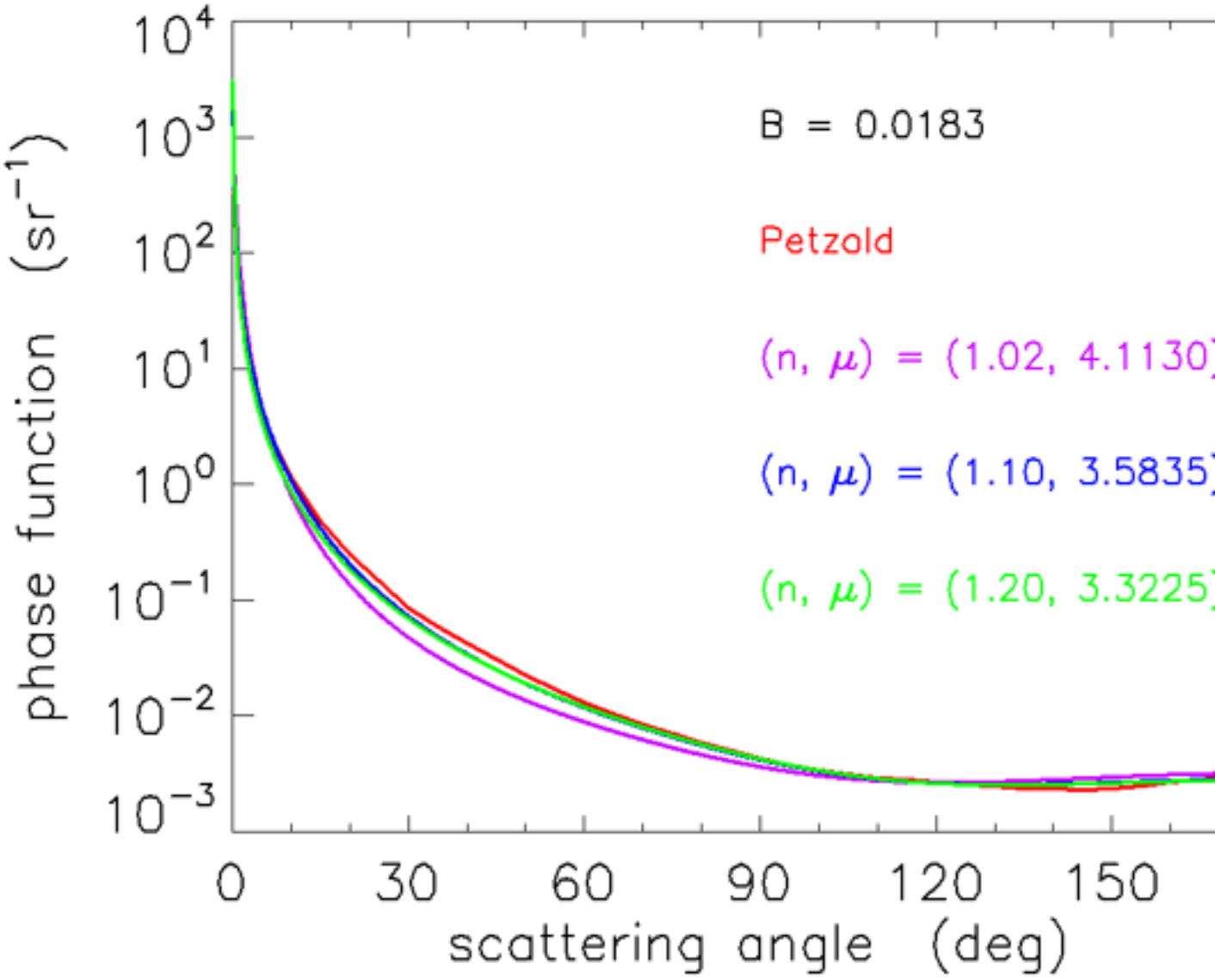

Figure 7: Log-linear plots of Fournier-Forand phase functions having the same backscatter fraction $B = 0.0183$ but generated by the three n, μ pairs shown by the red symbols in Fig. figure5. The Petzold average-particle phase function is shown in red.